Journal of Herpetology, Vol. 52, No. 2, 185–192, 2018

Spermatogenesis and Testicular Cycle in Rough Greensnakes, *Opheodrys aestivus*, from Arkansas

John D. Konvalina,[1,2] Stanley E. Trauth,[1] and Michael V. Plummer[3]

[1]*Department of Biological Sciences, Arkansas State University, PO Box 599, State University, Arkansas 72467 USA*
[3]*Department of Biology, Harding University, 915 E Market Avenue, Searcy, Arkansas 72143 USA*

Abstract.—**Spermatogenesis, the production of sperm, is a fundamental part of the reproductive cycle in vertebrates and warrants detailed study. Reptiles exhibit a hybrid pattern of spermatogenesis that has similarities with both anamniotes and amniotes. Researching this interesting transition will help us better understand vertebrate evolution. To this end, we histologically examined the spermatogenic and testicular cycle of Rough Greensnakes (*Opheodrys aestivus*) from Arkansas. We hypothesized that spermatogenesis in Rough Greensnakes would follow the different spermatogenic stages found in previously published studies on temperate snakes. In addition, we hypothesized that both season and seminiferous tubule diameter would have a significant effect on seminiferous tubule epithelial height. Finally, we hypothesized that Rough Greensnakes would exhibit postnuptial spermatogenesis. We constructed a cell wheel illustrating the chronological development of all germ cell stages for this species and measured seminiferous tubule diameter and seminiferous tubule epithelial height from 22 specimens. *Opheodrys aestivus* exhibited small seminiferous tubule diameters in spring followed by an increase in summer. By October the lumen was mostly empty of sperm because they had migrated to the vas deferens for winter storage. Seminiferous tubule epithelial height was significantly correlated with seminiferous tubule diameter. Both seminiferous tubule diameter and season significantly affected seminiferous tubule epithelial height. This species can be categorized as having postnuptial spermatogenesis where sperm are produced in the summer after spring mating. Future studies of *O. aestivus* need to investigate the testicular cycle in other parts of their geographic distribution to see if this monthly pattern is consistent.**

Spermatogenesis, the production of sperm, is a fundamental part of the reproductive cycle in vertebrates and warrants detailed study. Knowing when sperm are produced for a particular species will aid with captive breeding efforts if the species is ever in need of conservation. Species have both synchronous (male and female gametes produced at the same time) and asynchronous (male and female gametes produced at different times) reproductive cycles. Knowledge of these cycles will be essential in any attempts at captive breeding. Finally, the spermatogenic and testicular cycles are greatly affected by environmental temperatures (Hawley and Aleksiuk, 1976). Recognizing the optimal temperature at which to keep specimens or when to change the environmental temperature is crucial in maintaining these natural processes in artificial settings. Overall, comprehending the intricacies of the spermatogenic and testicular cycles in a species allows us to better aid conservation and breeding efforts.

Vertebrate spermatogenesis can be divided into two groups: cystic and acystic. Cystic spermatogenesis is diagnostic of anamniotes and is characterized by each seminiferous tubule within the testis housing multiple cysts. These cysts contain a population of germ cells that are all at the same stage of development. These cells progress through spermatogenesis as a cohort. Eventually the cyst ruptures and mature spermatozoa are emptied in the lumen (Gribbins, 2011). Amniotes have acystic spermatogenesis in which the different stages of spermatogenesis can be found within the seminiferous epithelium. Instead of cysts, the cohorts develop in tandem with Sertoli cells, which provide vital nutrition to the developing cells (Gribbins, 2011).

Birds and mammals exhibit a concurrent spatial germ cell development strategy in which every cell type is always present. This means that all the cells are concurrently part of the same generation (Gribbins, 2011). Reptiles have a temporal germ cell development strategy that is more similar to anamniotes than to other amniotes (Gribbins et al., 2005). Across the year, different germ cell types will be present in the seminiferous tubules of reptiles; however, these different germ cell types belong to different generations. In reptiles, germ cells develop as a cohort going from one stage to the next simultaneously. This results in each spermiation event being comprised of a different cohort. In other words, in reptiles different stages are produced at different times of the year, whereas in birds and mammals all stages are always present and a cell's position in the epithelium determines its stage. The closer is a cell to the lumen, the more advanced is its stage (Gribbins, 2011).

The anamniote–amniote hybrid pattern of spermatogenesis in reptiles (acystic with temporal germ cell development strategy) makes it an interesting one to study and can aid in our understanding of vertebrate evolution; however, few reptilian spermatogenic studies have been completed (Gribbins, 2011). In-depth analysis is needed on Sertoli cells, interstitial tissue, and germ cell development strategies. Sertoli cells are found in seminiferous tubules and nourish sperm cells through the process of spermatogenesis (França et al., 2016). Sperm morphology, especially ultrastructure data, is needed for many species of snakes (Gribbins and Rheubert, 2011); however, exemplary studies of ophidian spermatogenesis do exist. Elichi et al. (1994) found lipidlike structures implanted in the cytoplasm of elongated spermatids while analyzing seasonal spermatogenesis in Japanese Ratsnakes (*Elaphe climacophora*). They also found lipid droplets in Sertoli cells. In addition to Japanese Ratsnakes, these lipidlike structures already have been found in Crowned Snakes (*Tantilla coronata*), Boa Constrictors (*Boa constrictor*), and Habus (*Trimeresurus* spp.), suggesting that they may be a common feature to snake spermatids (Elichi et al., 1994). Spermatogenesis obviously differs greatly among species, thus warranting further study within ophidians.

[2]Corresponding Author. Present address: Department of Biology, University of Central Florida, 400 Central Florida Boulevard, Orlando, Florida 32816 USA; E-mail: jkonvalina@knights.ucf.edu
DOI: 10.1670/16-163

TABLE 1. *Opheodrys aestivus* specimens from Arkansas used for light microscopy. All sections taken were of the testis and prepared by SET. (HUC = Harding University Campus in Searcy, Arkansas, USA; JDW = J. D. Wilhide; MVP = Michael V. Plummer; RB = Roger Buchanan; SET = Stan E. Trauth.)

Catalogue number	Collection date	Preparation date	Snout–vent length (mm)	Tail length (mm)	Arkansas county	Specific location	Collector name
18994	15 MAY 1993	17 MAY 1993	N/A	N/A	Marion	vicinity of Old Buffalo Hwy 101	SET/RB/JDW
31269	18 OCT 2008	22 OCT 2008	323	212	N/A	N/A	Melissa Patrick and Josh Engelbert
31444	16 APR 2010	18 APR 2010	413	268	White	HUC	MVP
31445	16 APR 2010	18 APR 2010	448	283	White	HUC	MVP
31447	16 APR 2010	18 APR 2010	462	307	White	HUC	MVP
31519	14 MAY 2010	15 MAY 2010	405	276	White	HUC	MVP
31520	14 MAY 2010	15 MAY 2010	411	254	White	HUC	MVP
31521	14 MAY 2010	15 MAY 2010	353	206	White	HUC	MVP
31533	15 JUN 2010	17 JUN 2010	282	176	White	HUC	MVP
31534	15 JUN 2010	17 JUN 2010	400	278	White	HUC	MVP
31535	15 JUN 2010	17 JUN 2010	412	286	White	HUC	MVP
31539	17 JUL 2010	30 JUL 2010	291	196	White	Bald Knob Lake	MVP
31540	17 JUL 2010	30 JUL 2010	388	260	White	Bald Knob Lake	MVP
31541	17 JUL 2010	30 JUL 2010	420	296	White	Bald Knob Lake	MVP
31542	17 JUL 2010	30 JUL 2010	424	263	White	Bald Knob Lake	MVP
31551	2 SEP 2010	10 SEP 2010	331	213	White	HUC	MVP
31552	2 SEP 2010	10 SEP 2010	348	233	White	HUC	MVP
31553	2 SEP 2010	10 SEP 2010	347	216	White	HUC	MVP
32066	22 APR 2012	24 APR 2012	349	235	Perry	Fr 132 & 43B—site 15 ~ 1 m W Black	Herp class-SET
32136	22 APR 2012	2 MAY 2012	345	212	Montgomery	Springs on St Hwy 8—site 15	Herp class-SET
33375	25 AUG 2015	31 AUG 2015	420	285	White	Bald Knob Lake	MVP
33376	25 AUG 2015	31 AUG 15	410	240	White	Bald Knob Lake	MVP

Testicular cycles of initiation and recrudescence of gametes are still largely unknown in the suborder Serpentes (Gribbins, 2011). Mating strategies differ between snake species, with some exhibiting biannual breeding, whereas others are only annual breeders (Saint Girons, 1982). Western Cottonmouths (*Agkistrodon piscivorus leucostoma*), a semiaquatic snake species common to the southeastern United States, have two periods of spermatogenesis within the same calendar year (March–June and August–October), suggesting multiple breeding periods throughout the year (Gribbins et al., 2008).

Jadhav and Padgaonkar (2011) divide the testicular cycle in snakes into four parts: breeding (all stages of spermatogenesis are active), degeneration (cells start to die), regression (cessation of spermatogenesis), and recrudescence (reinitiation of spermatogenesis). These phases are triggered in part by seasonal changes (Hawley and Aleksiuk, 1976). In Red-Sided Gartersnakes (*Thamnophis sirtalis parietalis*), photoperiod has no impact on the recrudescence of testes, yet environmental temperature correlates with the initiation of spermatogenesis (Hawley and Aleksiuk, 1976). Goldberg and Parker (1975) found seasonal differences in testicular stages in two species of colubrid snakes (*Masticophis taeniatus* and *Pituophis melanoleucus*) by measuring interstitial cell nuclear diameters, seminiferous tubule diameters, and epithelial heights.

Some species, such as Eastern Gartersnakes (*Thamnophis sirtalis sirtalis*), store sperm over winter in the vas deferens (Clesson et al., 2002), whereas others such as Western Wormsnakes (*Carphophis vermis*) retain sperm within the ductus deferens year round (Aldridge and Metter, 1973). Chinese Ratsnakes (*Zaocys dhumnades*) store sperm in the vas deferens and also the epididymis (Liang et al., 2011). Comparing testis volume with the total mass of the organism is a good method for deciphering seasonal allocation of resources between somatic growth and reproduction (Moshiri et al., 2014).

Finally, Aldridge et al. (1990) revealed that spermatogenesis peaks in July using seasonal histology of the testis in Rough Greensnakes (*Opheodrys aestivus*). Regardless, this study did not visually identify the different stages of spermatogenesis, which are needed for comparison with other species. We addressed this problem in our study by chronologically recording the different stages of spermatogenesis in *O. aestivus*. We hypothesized that the same factors would affect spermatogenesis in Rough Greensnakes as they do other temperate species and therefore predicted the different stages of spermatogenesis to follow Gribbins (2011). In addition, we aimed to identify which factors affect seminiferous tubule epithelial height. We hypothesized that both season and seminiferous tubule diameter would have a significant effect on seminiferous tubule epithelial height. Therefore, we expected to find significant differences in seminiferous tubule epithelial height among seasons and among different seminiferous tubule diameters. We also hypothesized that Rough Greensnakes would exhibit postnuptial spermatogenesis, corroborating what Aldridge et al. (1990) found.

MATERIALS AND METHODS

We collected 22 snakes over a period of 22 yr (1993–2015; Table 1), with all but 2 of those snakes collected from 2010–2015. We removed the urogenital structures from these snakes and prepared them for light microscopy (LM). Testes were immediately placed into vials of 2% glutaraldehyde (GTA) solution buffered with 0.1 M sodium cacodylate at a pH of 7.2 and allowed to fix for 2 h. For postfixation, we used 1% osmium tetroxide, buffered as above, for 2 h. For LM, we fixed plastic-embedded testes in 2% GTA. Testes were then dehydrated in a graded series of increasing ethanol solutions (50–100%), placed in a 50%/50% acetone/plastic mixture for overnight infiltration, and embedded in Mollenhauer's Epon-Araldite #2 (Dawes, 1988). For thick sectioning (~1 μm in thickness) and staining, we

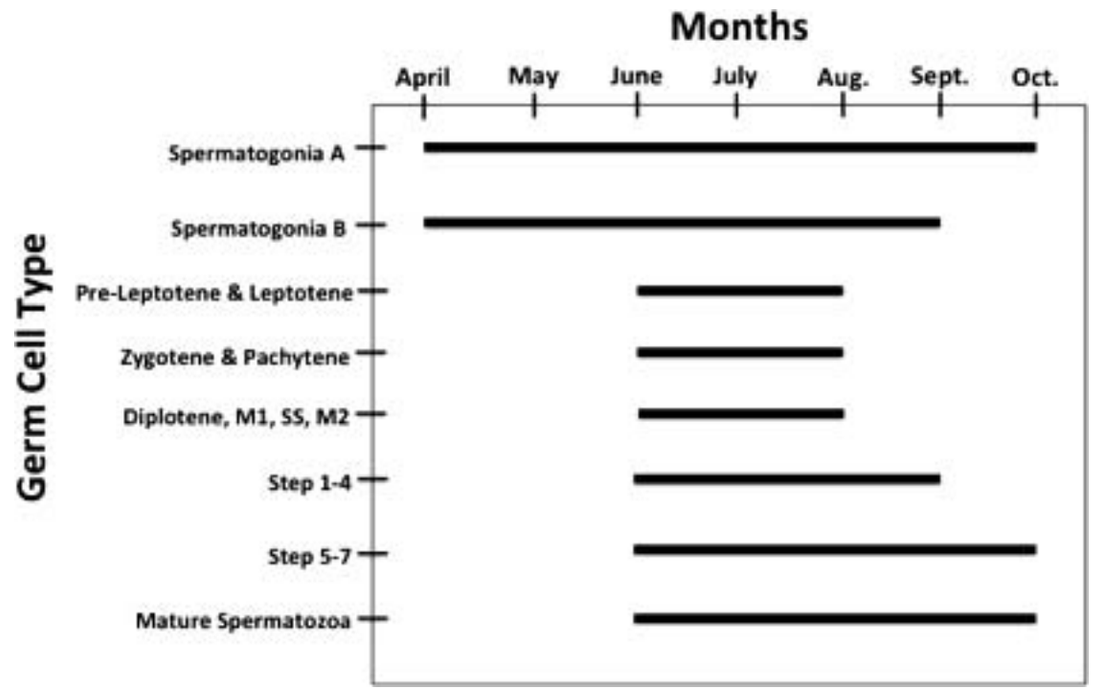

FIG. 1. Time and appearance of germ cell distribution within the seminiferous epithelium of *Opheodrys aestivus* collected in Arkansas, USA from 1993 through 2015. M1, metaphase 1; SS, secondary spermatocyte; M2, metaphase 2; steps 1–4 and steps 5–7, spermatid steps 1–7.

used glass knives on a type 4801A Ultrotome (LKB Instruments, Inc., Rockville, Maryland, USA) with Ladd® multiple stain, respectively. Ladd® multiple stain is a generic replacement for paragon epoxy tissue stain. For photomicroscopy, we utilized an Eclipse 600 epifluorescent light microscope with a DXM 1200C digital camera (Nikon Instruments Inc, Melville, New York, USA).

Our sample included individuals collected at various stages of the spermatogenic cycle. We photographed each stage to complete a cell wheel showing the entire spermatogenic cycle of Rough Greensnakes. For each specimen we haphazardly selected 20 seminiferous tubules and measured seminiferous tubule diameter and seminiferous epithelial height. Seminiferous tubule diameter was defined as the lumen plus the epithelium at the widest point of the tubule. Both seminiferous tubule diameter and seminiferous tubule epithelial height were measured in micrometers. We set the number of seminiferous tubules measured at 20, because it was the highest number of seminiferous tubules available for every specimen. We averaged the 20 measurements to give each individual an average seminiferous tubule diameter and average seminiferous tubule epithelial height. Because of small monthly sample sizes, we collapsed the months into three temporal groups: spring (April and May, $n = 9$), summer (June and July, $n = 7$), and fall (August–October, $n = 6$).

We used a Pearson correlation test to look for an association between seminiferous tubule diameter and seminiferous tubule epithelial height. To determine what factors influenced seminiferous tubule epithelial height we tested four linear models. The first was seminiferous tubule epithelial height as function of season; the second was seminiferous tubule epithelial height as a function of seminiferous tubule diameter; the third was seminiferous tubule epithelial height as a function of seminiferous tubule diameter plus season; and the final model was seminiferous tubule epithelial height as a function of seminiferous tubule diameter plus season plus an interaction between those two terms. We used the Akaike information criterion (AIC) (Akaike, 1973) to determine which model best fit the data. We then plotted the model with 95% confidence intervals by using the geom_smooth argument in the ggplot2 package. We performed all statistical analyses at a 5% significance level using the statistical programming software R (R Development Core Team, 2014).

RESULTS

Spermatogenesis can be divided into three distinct phases: proliferative, meiotic, and spermiogenic (Gribbins, 2011). Different germ cell types occur during different times of the year (Fig. 1). The following descriptions of germ cell stages were modeled after Gribbins (2011) and Lancaster et al. (2014).

Proliferative Stage.—This stage comprises two cell types: type A and B spermatogonia. Spermatogonia are the progenitor cells that mitotically divide to produce preleptotene spermatocytes. These cells line the basement membrane of the seminiferous tubules and can extend several layers thick into the lumen. Type A spermatogonia (Fig. 2, SpA) are oval shaped and line the basement membrane of seminiferous tubules. They are filled with diffuse chromatin and one or more nucleoli can clearly be seen within the nucleus. The second and final proliferative stage is comprised of type B spermatogonia (Fig. 2, SpB). These cells are rounder than type A spermatogonia and have condensed heterochromatin.

Meiotic Stage: Spermatocyte Morphology.—The start of the meiotic stage of spermatogenesis is evidenced by nuclear enlargement and condensation of chromatin in preparation for cellular division. Preleptotene spermatocytes (Fig. 2, PL) are the products of the mitotic division of type B spermatogonia. They appear similar to type B spermatogonia but can be distinguished by their smaller size and increased distance from the basement

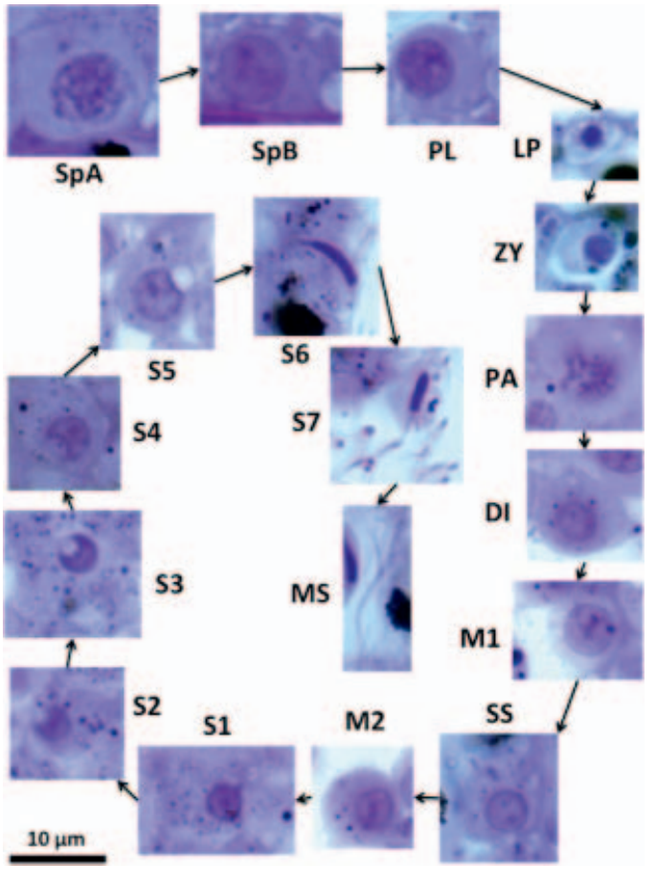

FIG. 2. Complete spermatogenic cycle for *Opheodrys aestivus* from Arkansas, USA, with the following germ cell types: type A spermatogonia (SpA), type B spermatogonia (SpB), preleptotene spermatocyte (PL), leptotene spermatocyte (LP), zygotene spermatocyte (ZY), pachytene spermatocyte (PA), diplotene spermatocyte (DI), metaphase 1 (M1), secondary spermatocyte (SS), metaphase 2 (M2), step 1 spermatid (S1), step 2 spermatid (S2), step 3 spermatid (S3), step 4 spermatid (S4), step 5 spermatid (S5), step 6 spermatid (S6), step 7 spermatid (S7), mature sperm (MS).

membrane. A major diagnostic characteristic of preleptotene cells is multiple dark-staining nucleoli.

In leptotene spermatocytes (Fig. 2, LP) heterochromatin condenses into threads of condensing chromosomes. Zygotene spermatocytes (Fig. 2, ZY) represent an increase in cell size and thickening of chromosomal fibers. This leads to the pairing of homologous chromosomes into tetrads. Pachytene spermatocytes (Fig. 2, PA) have very thick chromosomal fibers separated by large areas of nucleoplasm. Synaptonemal complexes are present, creating the area where crossing over events occur. Reptilian pachytene spermatocytes do not possess sex vesicles like their mammalian counterparts. The main function of the pachytene stage is to initiate genetic recombination.

The diplotene phase (Fig. 2, DI) is characterized by a degenerating nuclear membrane and a spokelike pattern of condensed chromosomal fibers arranged in a circle. Diplotene cells often are found in conjunction with metaphase I cells, secondary spermatocytes, and metaphase II cells. Diplotene cells form diploid primary spermatocytes. These cells undergo metaphase I (Fig. 2, M1) in which the chromosomes line up along the metaphase plate. After anaphase I and telophase I, two haploid secondary spermatocytes (Fig. 2, SS) are formed. Characteristics of secondary spermatocytes include a visible nuclear membrane, chromatin fibers dispersed through the nucleoplasm, vacuolated mitochondria, and a cytoplasmic amorphic inclusion called a nuage. These secondary spermatocytes undergo meiosis II, which includes metaphase II (Fig. 2, M2). Again, metaphase II cells are characterized by chromosomes lining up on the metaphase plate, but are half the size of metaphase I cells and have half the amount of chromatin.

TABLE 2. Mean ± standard error seminiferous tubule diameter and seminiferous tubule epithelial height by month from *Opheodrys aestivus* testes from Arkansas, USA.

Month	*n*	Mean diameter (µm)	Mean epithelial height (µm)
APR	5	136.22 ± 10.75	42.64 ± 1.72
MAY	4	119.65 ± 8.36	37.89 ± 4.73
JUN	3	226.63 ± 44.47	60.15 ± 13.6
JUL	4	301.88 ± 25.21	88.06 ± 14.17
AUG	2	254.98 ± 1.19	64.17 ± 5.21
SEP	3	235.98 ± 23.62	43.53 ± 1.48
OCT	1	147.46 ± 147.46	34.62 ± 34.62

Spermiogenic Stage: Spermatid Morphology.—Spermiogenesis, or the formation of mature spermatozoa from secondary spermatocytes, is comprised of seven steps. The first, a haploid step 1 spermatid (Fig. 2, S1), is the result of meiosis II. Step 1 spermatids are small, similar to the size of preleptotene spermatocytes. Defining characteristics include a well-defined nuclear membrane, a centrally located spherical nucleus, and no noticeable acrosome development. Step 2 spermatids (Fig. 2, S2) have a well-defined acrosomal vesicle and have chromatin dispersed throughout the nucleoplasm. Step 3 spermatids (Fig. 2, S3) have an acrosome that extends away from the apex of the nucleus. The acrosome of step 4 spermatids (Fig. 2, S4) surrounds the nucleus and begins to flatten it. In step 5 spermatids (Fig. 2, S5) the acrosome greatly increases in size and deeply embeds itself into a nuclear fossa. In step 6 spermatids (Fig. 2, S6) an elongation event begin to push the nucleus caudally and the acrosome vesicle is pushed up against the cell membrane. Step 7 spermatids (Fig. 2, S7) have completely condensed chromatin, a condensed nucleus, and elimination of much of the cytoplasm. The nuclei are densely stained and the flagellum begins to elongate. With a fully elongated flagellum, the step 7 spermatid becomes a mature spermatozoon (Fig. 2, MS) and is released into the lumen.

Testicular Histology.—There was a strong positive correlation between seminiferous tubule epithelial height and seminiferous tubule diameter ($r = 0.853$, df = 20, $P < 0.001$). Table 2 shows the mean ± standard error seminiferous tubule diameter and seminiferous tubule epithelial height by month. There is a steady increase to a peak in July followed by a subsequent decrease in both metrics in the fall. Figures 3 and 4 show this pattern broken down by season.

Model 3 (seminiferous tubule epithelial height ~ seminiferous tubule diameter + season) was the best model according to AIC (Table 3). The plot (Fig. 5) and summary (Table 4) of model 3 shows significant differences in seminiferous tubule epithelial height between spring and fall (df = 18, $P = 0.004$) and between summer and fall (df = 18, $P = 0.0256$). Likewise, seminiferous tubule diameter has a significant effect (df = 18, $P < 0.001$). Model 4 (seminiferous tubule epithelial height ~ seminiferous tubule diameter × season) had a ΔAIC of 1.2 and therefore is commensurate with model 3.

We photographed the monthly variation in seminiferous tubule diameter and seminiferous tubule epithelial height (Fig. 6). The photos shown are cross-sections of the testis showing

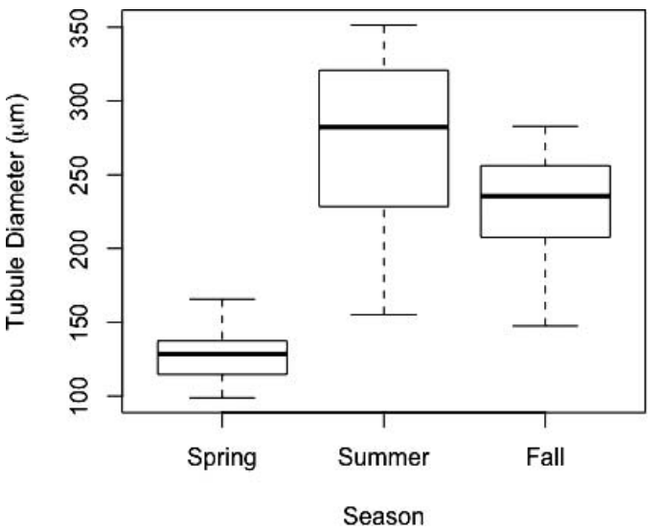

FIG. 3. Average seminiferous tubule diameter by season for *Opheodrys aestivus* from Arkansas, USA. The black horizontal line within each box represents the median value. The bottom and top of each box represent the first and third quartiles, respectively. Finally, the "whiskers" above and below the box show the maximum and minimum values.

multiple seminiferous tubules. These tubules are separated by interstitial tissue. The basement membrane is lined with Sertoli cells that nurse the primitive germ cells, types A and B spermatogonia.

DISCUSSION

The testes of *O. aestivus* are comprised of intertwining seminiferous tubules lined with an epithelium of different germ cell types (Fig. 6). During spring months, they contain only germ cells in the proliferative stage. Spermiation occurs in the summer months with all germ cell types present. In September, only the proliferative stages, spermatid stages, and mature spermatozoa were present. This continued in October where

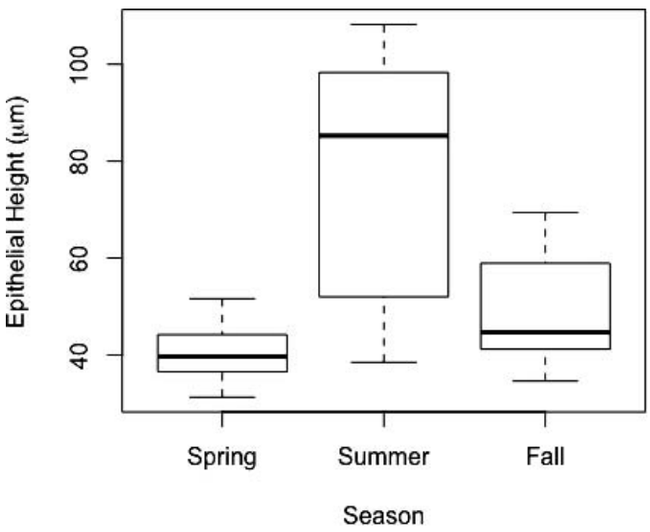

FIG. 4. Average seminiferous tubule epithelial height by season for *Opheodrys aestivus* from Arkansas, USA. Box plot description is the same as that in Figure 3.

TABLE 3. AIC table comparing linear models examining the factors contributing to seminiferous tubule epithelial height in *Opheodrys aestivus* from Arkansas, USA (EH = epithelial height; TD = tubule diameter; S = season).

	ΔAICc	df	AIC weight
EH ~ TD + S	0	5	0.631
EH ~ TD × S	1.2	7	0.344
EH ~ TD	6.4	3	0.025
EH ~ S	24.5	4	<0.001

only spermatogonia A, some spermatid stages, and mature spermatozoa are present. When spermatogenesis stops in the winter, the sperm are stored in the vas deferens to be used during spring mating (Aldridge et al., 1990). Observation of these stages confirmed our hypothesis that the spermatogenic cycle in *O. aestivus* would follow the temperate snakes reviewed in Gribbins (2011).

With this information, we can divide the spermatogenic cycle of *O. aestivus* into the following phases: recrudescence (April and May), breeding (June–August), degeneration (September and October), and regression (November–March). By producing sperm after they mate, *O. aestivus* can be classified as having postnuptial spermatogenesis. This confirms our hypothesis and corroborates what Aldridge et al. (1990) found. In addition, this pattern is consistent with other temperate reptiles (Gribbins, 2011). Another colubrid, Red-Sided Gartersnake (*T. sirtalis parietalis*), has a similar spermatogenic cycle where it stores sperm in the ductus deferens during winter and then breeds immediately after emerging from hibernation (Garstka et al., 1982).

Rough Greensnakes have only one peak in spermiogenesis, which supports the idea that they are annual breeders, unlike biannual breeding Cottonmouths (Gribbins et al. 2008). No lipidlike structures were found in the Sertoli cells, such as those found in Elichi et al. (1994).

Seminiferous tubule diameter was small in spring and then increased in summer. Tubule diameter decreased in fall. By October, the lumen was mostly empty of sperm since they migrated to the ductus deferens for winter storage. Epithelial height followed an identical pattern as tubule diameter, with

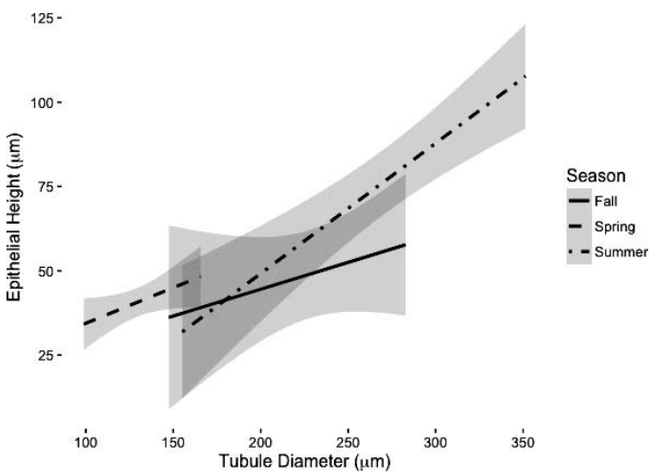

FIG 5. Plot of best model (seminiferous tubule epithelial height ~ seminiferous tubule diameter + season) for explaining the factors that affect seminiferous tubule epithelial height in *Opheodrys aestivus* from Arkansas. Shaded areas represent 95% confidence intervals.

TABLE 4. Summary of best model (seminiferous tubule epithelial height ~ seminiferous tubule diameter + season) for explaining the factors that affect seminiferous tubule epithelial height in *Opheodrys aestivus* from Arkansas, USA. Intercept is the value of seminiferous tubule epithelial height with a seminiferous tubule diameter of zero during fall.

	Estimate	SE	*t* value	*P* value
Intercept	−22.271	11.243	−1.981	0.063
Tubule diameter	0.313	0.046	6.77	<0.001
Spring	22.487	6.878	3.274	0.004
Summer	14.012	5.758	2.433	0.026

small values in spring, an increase in summer, and a subsequent decrease in fall. Peak length in seminiferous tubule diameter matched peak spermiation levels, which corroborates the findings with Chinese Skinks (*Eumeces chinensis*) (Hu et al., 2004).

The best model to predict seminiferous tubule epithelial height was an additive model of season plus seminiferous tubule diameter. When looking at the plot of the model (Fig. 5), there are clear and significant differences in seminiferous tubule epithelial height among seasons. The increased slope for summer may indicate a slight interactive effect between season and seminiferous tubule diameter as the model that included the interaction term (model 4) was within two AIC units of the additive model (model 3). On the basis of these results we can accept our hypothesis that seminiferous tubule epithelial height is affected by both seminiferous tubule diameter and season.

All snakes used in this study with the exception of two were collected in a 5-yr timespan (2010–2015). Differences in health of individuals could have been caused by environmental variation (temperature, precipitation) as well as varying prey availability across this timespan. This could in turn affect the spermatogenic cycle of each individual. Therefore the scope of the inference of this study is bound by these limitations. In the coming decades, climate change could alter these cycles. Warmer autumns could lead to the lengthening of the spermatogenic cycle and delaying of regression until early winter. Likewise, recrudescence could start at earlier and earlier times. In Red-Sided Gartersnakes (*T. sirtalis parietalis*), photoperiod has no impact on the recrudescence of testes, but environmental temperature correlates with the initiation of spermatogenesis (Hawley and Aleksiuk, 1976). If true in other colubrids, this would mean that all temperate snakes, no matter their latitude, would experience an earlier recrudescence period. Taken to the extreme, one could imagine

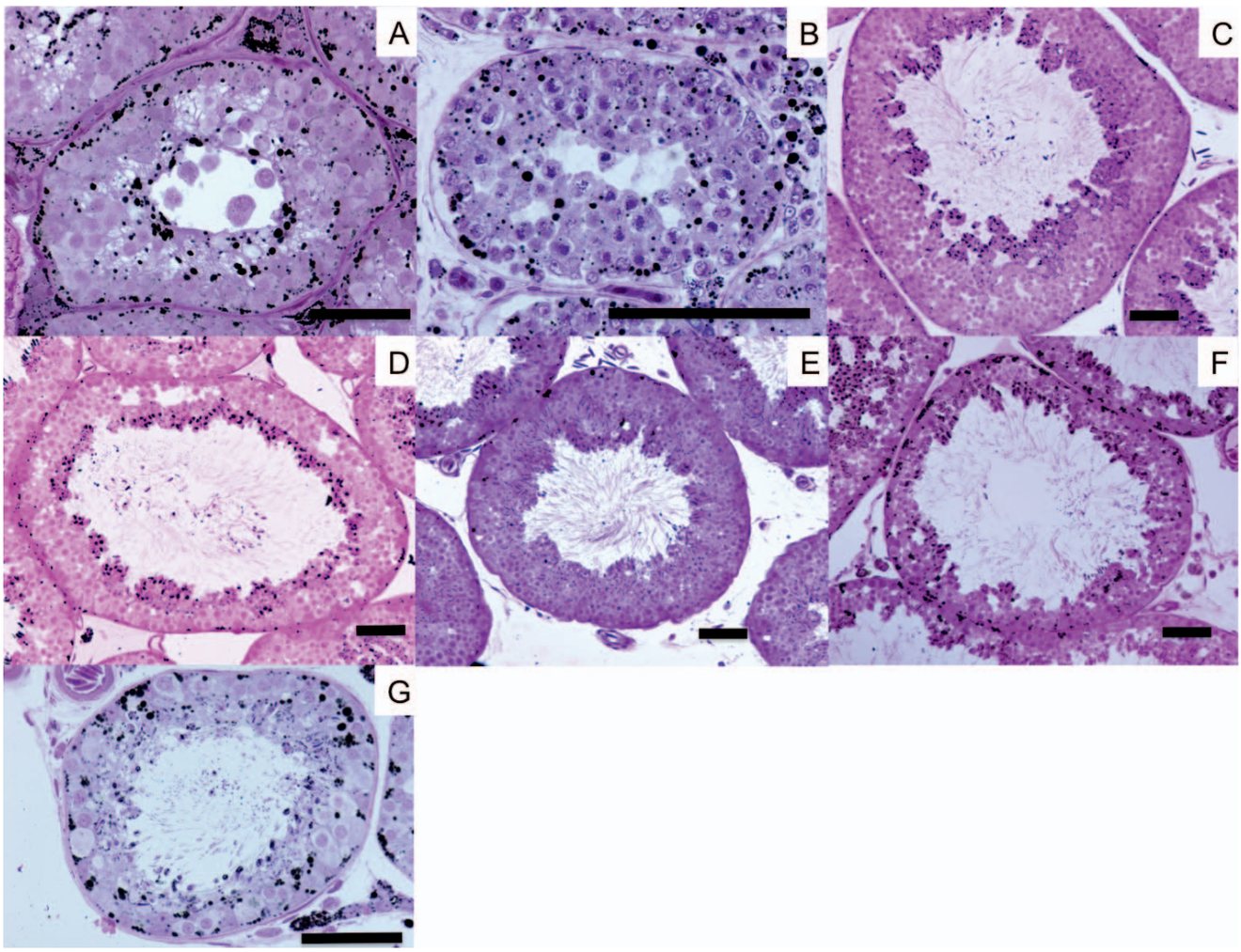

FIG. 6. Representative cross-sections of seminiferous tubules from *Opheodrys aestivus* from Arkansas for the following months: April (A), May (B), June (C), Juuly (D), August (E), September (F), and October (G). Bar = 50 μm. Staining method used: Ladd® multiple stain.

snakes in the southern United States adopting a continuous spermatogenic cycle if temperatures became consistently warm enough to eliminate the need for hibernation. Future studies should investigate this pattern at the fringes of Rough Greensnakes' range, the tip of the Florida peninsula in the south and southern New Jersey in the north, to see if these patterns are consistent across all populations.

Acknowledgments.—We thank V. Rolland for assistance with R software and statistical analyses. We also thank J. Bouldin and T. McKay for help with revising and editing this manuscript. The Arkansas Game and Fish Commission provided Scientific Collecting Permits to SET and MVP. See Appendix 1 for yearly permit numbers. All aspects of this research were approved by the Harding University Animal Care Committee and were conducted following established guidelines for reptilian field research (http://www.asih.org/sites/default/files/ documents/Resources/guidelinesherpsresearch2004.pdf).

Literature Cited

Akaike, H. 1973. Information theory as an extension of the maximum likelihood principle. Pp. 267–281 in B. N. Petrov and F. Csaki (eds.), Second International Symposium on Information Theory. Akademinai Kiado, Budapest, Hungary.

Aldridge, R. D., and D. E. Metter. 1973. The reproductive cycle of the western worm snake, *Carphophis vermis*, in Missouri. Copeia 1973: 472–477.

Aldridge, R. D., J. J. Greenhaw, and M. V. Plummer. 1990. The male reproductive cycle of the rough green snake (*Opheodrys aestivus*). Amphibia-Reptilia 11:165–173.

Clesson, D., A. Bautista, D. D. Baleckaitis, and R. W. Krohmer. 2002. Reproductive biology of male eastern garter snakes (*Thamnophis sirtalis sirtalis*) from a denning population in central Wisconsin. American Midland Naturalist 147:376–386.

Dawes, C. J. 1988. Introduction to Biological Electron Microscopy: Theory and Techniques. Ladd Research Industries, Inc., USA.

Elichi, H., K. Masamichi, T. Michihisa, and Y. Hayashi. 1994. Seasonal changes in spermatogenesis and ultrastructure of developing spermatids in the Japanese rat snake, *Elaphe climacophora*. Journal of Veterinary Medical Science 56:835–840.

França, L. R., R. A. Hess, J. M. Dufour, M. C. Hofmann, and M. D. Griswold. 2016. The Sertoli cell: one hundred years of beauty and plasticity. Andrology 4:189–212.

Garstka, W. R., B. Camazine, and D. Crews. 1982. Interactions of behavior and physiology during the annual reproductive cycle of the red-sided garter snake (*Thamnophis sirtalis parietalis*). Herpetologica 38:104–123.

Goldberg, S. R., and W. S. Parker. 1975. Seasonal testicular histology of the colubrid snakes, *Masticophis taeniatus* and *Pituophis melanoleucus*. Herpetologica 31:317–322.

Gribbins, K. M. 2011. Reptilian spermatogenesis: a histological and ultrastructural perspective. Spermatogenesis 1:250–269.

Gribbins, K. M., and J. L. Rheubert. 2011. The ophidian testis, spermatogenesis, and mature spermatozoa. Pp. 183–264 in D. M. Sever and R. D. Aldridge (wds.), Reproductive Biology and Phylogeny of Snakes. Science Publishers, Inc., USA.

Gribbins, K. M., C. S. Happ, and D. M. Sever. 2005. Ultrastructure of the reproductive system of the black swamp snake (*Seminatrix pygaea*). Acta Zoologica 86:223–230.

Gribbins, K. M., J. J. Rheubert, M. H. Collier, D. S. Siegel, and D. M. Sever. 2008. Histological analysis of spermatogenesis and the germ cell development strategy within the testis of the male western cottonmouth snake, *Agkistrodon piscivorus leucostoma*. Annals of Anatomy 190:461.

Hawley, A. W. L., and M. Aleksiuk. 1976. The influence of photoperiod and temperature on seasonal testicular recrudescence in the red-sided garter snake (*Thamnophis sirtalis parietalis*). Comparative Biochemistry and Physiology 53:215–221.

Hu J., J. Du, and X. Ji. 2004. Annual variation in gonads of male Chinese skinks *Eumeces chinensis*. Acta Zoologica Sinica 50:103–110.

Jadhav, R. N., and A. S. Padgaonkar. 2011. Seasonal male reproductive cycle of the estuarine snake *Enhydris enhydris* Schneider. Journal of Endocrinology and Reproduction 15:37–42.

Lancaster, K., S. E. Trauth, and K. M. Gribbins. 2014. Testicular histology and germ cell cytology during spermatogenesis in the Mississippi map turtle, *Graptemys pseudogeographica kohnii,* from Northeast Arkansas. Spermatogenesis 4:e992654.

Liang, G., L. Qiao-Qiao, Y. Hu-Hu, and Q. Wang. 2011. Histological and immunocytochemical study of deferens ducts in the Chinese rat snake (*Zaocys dhumnades*). Zoological Research 3:663–669.

Moshiri, M., F. Todehdehghan, and A. Shiravi. 2014. Study of sperm reproductive parameters in mature Zanjani viper. Cell Journal 16: 111–116.

R Core Team. 2014. R: A language and environment for statistical computing. R Foundation for Statistical Computing, Vienna, Austria. Available from: http://www.R-project.org/.

Saint Girons, H. S. 1982. Reproductive cycles of male snakes and their relationships with climate and female reproductive cycles. Herpetologica 38:5–16.

Accepted: 27 February 2018.
Published online: 4 May 2018.

APPENDIX 1. Yearly permit numbers for the collection of *Opheodrys aestivus* from Arkansas, USA. No permits were required before 2004.

Year	Permit number
2015	012220145
2014	020520123
2013	020320123
2012	120820101
2011	120820101
2010	100220094
2009	080720081
2008	061420071
2007	042020062
2006	041120054
2005	041420042
2004	108201102003091941